As of 10 June 2016

This GOES-R Level 2+ space weather Algorithm Theoretical Basis Document (ATBD) is preliminary and subject to change as the GOES-R Program prepares for a launch in late 2016.

The NOAA National Centers for Environmental Information (NCEI) is currently developing a demonstration version of the Satellite Product Analysis and Distribution Enterprise System (SPADES) which will host the L2+ algorithms. The operational SPADES will be instantiated by the National Weather Service in FY2017 to serve the needs of the Space Weather Prediction Center (SWPC).

Updated versions of the L2+ ATBDs will periodically be made available and posted to the SPADES website.

Bill Denig
NCEI

http://www.ngdc.noaa.gov/stp/space-weather/online-publications/stp_sii/spades/

NOAA NESDIS
National Geophysical Data Center

GOES-R SEISS.20 SOLAR PROTON EVENT RATE-OF-RISE ALGORITHM THEORETICAL BASIS DOCUMENT
Version 1.1

Hardcopy Uncontrolled

TITLE: SEISS.20 SOLAR PROTON EVENT RATE-OF-RISE
ALGORITHM THEORETICAL BASIS DOCUMENT VERSION 1.1

AUTHORS:
Juan V. Rodriguez

APPROVAL SIGNATURES:

_____ <Actual Signature Date>
Terrance G. Onsager
SEISS Instrument Scientist

_____ <Actual Signature Date>
William Denig
NGDC Principal Investigator

_____ <Actual Signature Date>
Steven Goodman
GOES-R Chief Scientist

SEISS.20 SOLAR PROTON EVENT RATE-OF-RISE ALGORITHM THEORETICAL BASIS DOCUMENT VERSION HISTORY SUMMARY

Revision Number	**Date**	**Author**	**Revision Description**	**Reason for Revision**
1.0	June 3, 2013	Juan V. Rodriguez	Initial release	CDR
1.1	May 20, 2014	Juan V. Rodriguez	Moved req'ts to Appendix A. Minor changes and corrections resulting from science code completion.	Science code completion

TABLE OF CONTENTS

LIST OF FIGURES 8
LIST OF TABLES 10
LIST OF ACRONYMS 11
ABSTRACT 12
1.0 INTRODUCTION 13
1.1 Purpose of This Document 13
1.2 Who Should Use This Document 13
1.3 Inside Each Section 13
1.4 Related Documents 14
1.5 Revision History 14
2.0 OBSERVING SYSTEM OVERVIEW 15
2.1 Product Generated 15
2.2 Instrument Characteristics 15
3.0 ALGORITHM DESCRIPTION 17
3.1 Algorithm Overview 17
3.2 Processing Outline 19
3.3 Algorithm Input 19
3.3.1 Primary Data 19
3.3.2 Ancillary Data 20
3.4 Theoretical Description 20
3.4.1 Physics of the Problem 20
3.4.2 Mathematical Description 21
3.4.3 Algorithm Output 26
4.0 TEST DATA SETS AND OUTPUTS 28
4.1 Simulated/Proxy Input Data Sets 28
4.2 Test Results Using Proxy Input Data 31
5.0 PRACTICAL CONSIDERATIONS 37
5.1 Numerical Computation Considerations 37
5.2 Programming and Procedural Considerations 37
5.3 Quality Assessment and Diagnostics 37
5.4 Exception Handling 37
5.5 Algorithm Validation 37
6.0 ASSUMPTIONS AND LIMITATIONS 37
6.1 Constants to be Re-evaluated During Cal/Val 37
6.2 Input and Output File Contents and Formats 38
6.3 Performance 38
6.4 Pre-Planned Product Improvements 38
7.0 REFERENCES 39
APPENDIX A. REQUIREMENTS. 41

LIST OF FIGURES

Figure 1. Cartoon of solar proton observations in the equatorial plane by westward- and eastward-looking detectors on GOES. A westward (eastward) detector observes protons whose gyrocenters like outside (inside) geostationary orbit. The arrows to the left indicate the solar protons propagating along the interplanetary magnetic field direction. The westward observations are much more likely than the eastward observations to accurately represent the solar proton flux levels outside Earth's magnetosphere at 1 AU. 16
Figure 2. Examples of solar proton event (SPE) onsets in which the quasi-exponential rise out of the noisy background appears approximately linear on a semi-logarithmic plot... 17
Figure 3. Example of a proxy output file for the onset of the Bastille Day 2000 event at >10 MeV.. 27
Figure 4. Example of a proxy output file for the onset of the Bastille Day 2000 event at >100 MeV.. 27
Figure 5. Comparison of eastward-observed (GOES-10) and westward-observed (GOES-12) fluxes with those observed from a spinning satellite (GOES-11). Observations are from the P2 (4.2-8.7 MeV) GOES channel. The oscillations in the GOES-11 fluxes are signatures of the flux anisotropies that result in the large differences between the GOES-10 and GOES-12 fluxes. 30
Figure 6. Integral fluxes during the rise of the 20 January 2005 event. The red traces are the proxy data calculated from the 1-min GOES-12 and GOES-11 data after removal of backgrounds and contamination. The black dotted traces indicate the results without removal of the backgrounds and contamination. The blue stars are the 5-min GOES-11 integral fluxes. The lower 5-min GOES-11 >10 MeV fluxes prior to event onset are due to the anisotropy averaging shown in Figure 5. 30
Figure 7. Rate-of-rise calculations for the 20 January 2005 event. The red trace is the 1-minute integral flux calculated by the L2 Integral Flux algorithm. The green trace is the running mean plus 3 sigma, which is used to detect a rapid rise in the presence of noise. The blue trace is the normalized backwards difference calculated from the running mean plus 3 sigma (the dashed blue trace is the criterion). The purple lines are the exponential fits to 4 consecutive points that meet or exceed the criterion, and the orange crosses are the corresponding time constants in minutes. 32
Figure 8. Rate-of-rise calculation for the 10 June 2000 event. See Figure 7 caption for explanation. 33
Figure 9. Rate-of-rise calculation for the 14 July 2000 event. See Figure 7 caption for explanation. 33
Figure 10. Rate-of-rise calculation for the 2 Nov 2003 event. See Figure 7 caption for explanation. 34
Figure 11. Rate-of-rise calculation for the 13 Dec 2006 event. See Figure 7 caption for explanation. 34

Figure 12. Rate-of-rise calculation for the 19 Oct 1989 event. See Figure 7 caption for explanation. 35
Figure 13. Rate-of-rise calculation for the 22 Oct 1989 event. See Figure 7 caption for explanation. 36

LIST OF TABLES

Table 1. Level 2 Integral Flux inputs to SEISS Solar Proton Event Rate-of-Rise algorithm. This is for each SGPS (–X and +X). 20
Table 2. Level 2 Outputs of SEISS Solar Proton Event Rate-of-Rise Algorithm. This is for each SGPS (–X and +X). 26
Table 3. Parameters Used in Removal of Backgrounds from 1-min Channel Fluxes 28
Table 4. Sources of Rate-of-Rise 1-minute Proxy Data 29
Table 5. Rapidly-rising events during Solar Cycle 23 and their onset times (UT) at each energy. 31
Table 6. Pre-Launch Values of the Configurable Constants in Solar Proton Rate-of-Rise Algorithm 38

LIST OF ACRONYMS

ATBD	Algorithm Theoretical Basis Document
AWG	Algorithm Working Group
CIRES	Cooperative Institute for Research in Environmental Sciences
eV	electron volt
FOV	field-of-view
JSC	Johnson Space Center (NASA)
keV	kilo-electron-volt
L1b	Level 1b
L2	Level 2
MeV	mega-electron-volt
NGDC	National Geophysical Data Center
pfu	particle flux unit
PORD	Performance and Operational Requirements Document
SEISS	Space Environment In-Situ Suite
SEP	solar energetic particle
SGPS	Solar and Galactic Proton Sensor
SPE	solar proton event
SRAG	Space Radiation Analysis Group
SWPC	Space Weather Prediction Center

ABSTRACT

The L2+ Solar Proton Event Detection algorithm operates on 5-min-cadence solar proton integral fluxes. Some solar proton events (SPEs) rise too rapidly for the Event Detection algorithm to provide sufficient advance warning. The L2+ Rate-of-Rise algorithm addresses this capability gap by operating on 1-min-cadence >10 MeV and >100 MeV integral fluxes. It estimates the rate-of-rise using an exponential fit to the 1-min fluxes and uses this rate-of-rise to predict when the event will reach different levels on the NOAA Solar Radiation Storm Scale (SRSS). The chief challenge is detecting true rapid event rises in the presence of noise without an excessive rate of false positives. This challenge is overcome by comparing a smoothed version of the fluxes to a pre-set, fixed criterion. Including this criterion, several parameters can be adjusted in order to balance the number of rapid events detected and the number of false positives. The algorithm has been tested using proxy data derived from 16 years of GOES data, using a criterion that the event rise more rapidly than one decade in 30 minutes. During this period, 33 rapidly-rising events were detected according to this criterion, with a false positive rate of 0.625 yr^{-1}. A faster criterion would result in fewer reported rapidly-rising events but also fewer false positives.

1.0 INTRODUCTION

1.1 Purpose of This Document

The purpose of this document is to describe the development and design of the SEISS algorithm produced to estimate the rate-of-rise of a solar proton event (SPE) from 1-minute-cadence fluxes, including details needed for implementation of the algorithm and examples of use and validation. It provides the operational requirements for this product and defines how these requirements are met with this algorithm. The algorithm inputs, processing and outputs are described in enough detail to design, develop, test and implement the necessary processing software and storage mechanisms.

1.2 Who Should Use This Document

The primary readership for this document includes those who have to implement the algorithm and those who seek to understand how the algorithm works and what its assumptions and limitations are. Members of the SWPC Space Weather Forecast Office should also use this ATBD to verify that their operational requirements are being met by the algorithm.

1.3 Inside Each Section

Section 2.0 OBSERVING SYSTEM OVERVIEW:
Describes the SEISS SGPS instrument and the measurements that serve as input to the algorithm.

Section 3.0 ALGORITHM DESCRIPTION:
Describes the development, theory and mathematics of the algorithm. Describes the logical flow of the algorithm, including input and output flow.

Section 4.0 TEST DATA SETS AND OUTPUTS:
Describes the test data sets used to characterize the performance of the algorithm and the data product quality. Describes the results from the algorithm processing on simulated input data.

Section 5.0 PRACTICAL CONSIDERATIONS:
Discusses issues involving numerical computation, programming and procedures, quality assessment and diagnostics and exception handling.

Section 6.0 ASSUMPTIONS AND LIMITATIONS:
Describes assumptions regarding input data contents and formats; instrument performance and characterization data; and potential future changes and improvements.

Section 7.0 REFERENCES:
Provides all references mentioned in the ATBD.

Appendix A REQUIREMENTS
Specifies the requirements for this algorithm.

1.4 Related Documents

GOES-R SEISS Differential-to-Integral Flux ATBD, Version 1.0, November 6, 2009.

GOES-R Series Mission Requirements Document (MRD), P417-R-MRD-0070, Version 3.13, August 2, 2011.

Space Environment In-Situ Suite (SEISS) Performance and Operational Requirements Document (PORD), 417-R-SEISSPORD-0030, Baseline Version 2.9, November 12, 2010.

1.5 Revision History

See p. 5.

2.0 OBSERVING SYSTEM OVERVIEW

2.1 Product Generated

The SWPC Space Weather Forecast Office uses GOES integral proton fluxes for operational solar radiation storm warnings and event alerts according to the solar radiation storm scale [Poppe, 2000]. (Integral fluxes represent the sum of fluxes in all instrument channels above a specified energy threshold.) The >10 MeV integral fluxes support warnings and alerts for robotic and human space flight. In addition, the >100 MeV integral fluxes support warnings and alerts for suborbital human flights, including commercial transpolar airline routes. The GOES-R Solar Proton Event (SPE) Detection product, which will support SWPC's issuance of solar radiation storm warnings and alerts, ingests L2 Integral Fluxes at a 5-minute cadence.

In addition to the Event Detection product, which provides continuity with current capabilities, SWPC has specified a new Rate-of-Rise product that is based on 1-minute-cadence integral fluxes. The purpose of this product is to provide a rapid alert of SPEs that rise too rapidly for the legacy Event Detection algorithm to provide sufficient advance warning. Knowing the rate of rise of events at their onset enables a rough projection of when the event will reach different levels on the solar radiation storm scale (SRSS), plus an additional 1000 pfu level for the >100 MeV fluxes (based on the 20 January 2005 event).

Although it is technically part of the Event Detection product, the Rate-of-Rise product is produced independently, and on a 1-min rather than 5-min cadence. Because of this independence, the Rate-of-Rise algorithm has its own ATBD. This separation improves the clarity of both the Rate-of-Rise and the Event Detection ATBDs.

2.2 Instrument Characteristics

The SEISS operational requirements and characteristics are detailed in section 3.3.6.1 of the GOES-R Series Mission Requirements Document (MRD, P417-R-MRD-0070) and the SEISS Performance and Operational Requirements Document (PORD, 417-R-SEISSPORD-0030). The requirements pertaining specifically to solar protons, which are pertinent to the rate-of-rise algorithm, are in section 3.3.6.1.4 of the MRD and 3.2.3 of the PORD.

SEISS is a suite of five particle sensors: magnetospheric particle sensors in a low-energy and high-energy range (MPS-LO and -HI), two solar and galactic proton sensors (SGPS), and an energetic heavy ion sensor (EHIS). The SGPS measures proton fluxes in ten

evenly spaced logarithmic energy bands from 1 MeV to 500 MeV and in an integral band above 500 MeV. One SGPS looks east and one looks west, as with the GOES 13-15 EPEAD. The westward FOV is the primary FOV for alerts and warnings because it observes proton fluxes whose gyrocenters lie outside geosynchronous orbit and therefore are more likely to be similar to the interplanetary fluxes (Figure 1). Because of different geomagnetic cutoffs for the two directions, the eastward-observed solar proton fluxes are usually lower than the westward-observed fluxes [Rodriguez et al., 2010]. Having two FOVs provides redundancy as well as a westward view regardless of spacecraft yaw flip status. This algorithm operates on the fluxes from both the westward and the eastward FOVs, but the forecast office will probably only use reports from the westward FOV, as determined by a yaw flip flag.

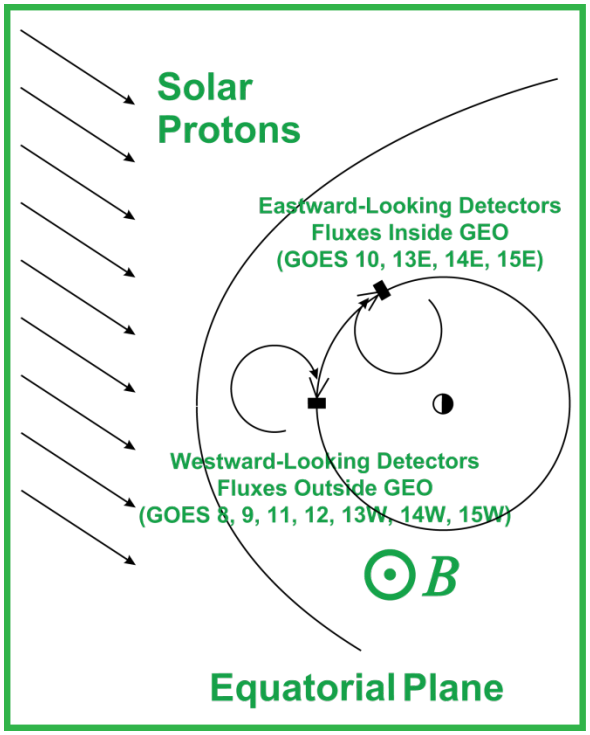

Figure 1. Cartoon of solar proton observations in the equatorial plane by westward- and eastward-looking detectors on GOES. A westward (eastward) detector observes protons whose gyrocenters like outside (inside) geostationary orbit. The arrows to the left indicate the solar protons propagating along the interplanetary magnetic field direction. The westward observations are much more likely than the eastward observations to accurately represent the solar proton flux levels outside Earth's magnetosphere at 1 AU.

3.0 ALGORITHM DESCRIPTION

3.1 Algorithm Overview

Many solar proton events (SPEs) rise sufficiently slowly that the legacy event detection algorithm is sufficient for issuing alerts against the solar radiation storm scale. However, the rapid rise of some events poses a hazard that the legacy algorithm is not designed to detect. The purpose of the SPE rate-of-rise algorithm is to provide a real-time alert to a rapid initial rise. It is not designed to predict when the event will peak. Event peaks generally occur after the rate-of-rise has decreased and are affected by interplanetary solar wind plasma structures as well as the behavior and location of the source.

The fundamental physical assumption of this algorithm is that an event rise resembles a rising exponential function. On the semi-logarithmic plots of integral flux produced daily by SWPC, SPEs rising out of a noisy but otherwise slowly-varying background level often appear to have a linear onset (Figure 2). This indicates that the SPE rise is approximately exponential in time. This fact has been used previously in characterizing the initial increase in solar proton fluxes [Posner, 2007]. Therefore, in this algorithm, the rates-of-rise are estimated based on an exponential fit.

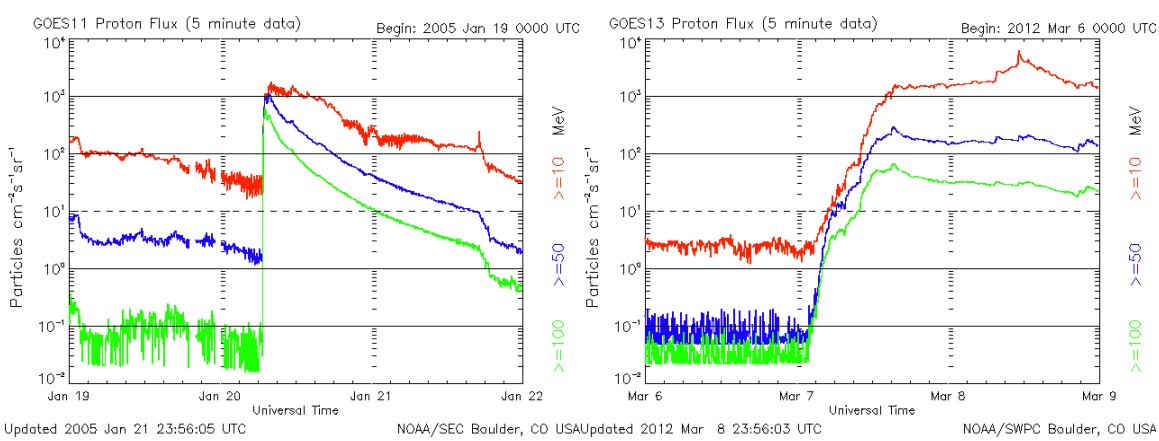

Figure 2. Examples of solar proton event (SPE) onsets in which the quasi-exponential rise out of the noisy background appears approximately linear on a semi-logarithmic plot.

The development of a real-time rate-of-rise algorithm faces several practical challenges:

1. Due to the importance of this product to alerts, a rate-of-rise has to be estimated in real-time based on only a few points. The event rise may be very rapid. For example, on 20 January 2005, the >100 MeV flux increased by more than 3 decades in 15 minutes, amounting to a rise time to peak of <20 minutes. This event posed a health risk to astronauts because of its rapid rise and very hard fluxes [Kim et al., 2005]. However,

solar proton integral fluxes are currently produced at a 5-minute cadence, which limits the ability to detect such rapid rises.

2. The instrument background level, out of which SPEs often rise, is very noisy, often in the range of a few counts per sample. Therefore, the algorithm must be capable of detecting a true rapid slope increase in the presence of noise.
3. Sometimes, a new SPE is superposed on a preexisting SPE (as in the 20 January 2005 case). Therefore, the detection method must be independent of the flux level at onset (unlike the Event Detection algorithm).
4. There is a sharp break in the slope (on a semi-log plot) at event onset. Therefore, the exponential fit cannot start until the event has started.

To address these challenges, we take the following approach:

1. We specify that the L2 Integral Flux product will be calculated on 1-minute cadences using 1-minute averages of L1b fluxes. The baseline 5-minute-cadence integral flux product needs to be continued, in part not to disrupt legacy products such as D-RAP [Sauer and Wilkinson, 2008] that rely on the 5-minute cadence. Therefore, the Integral Flux algorithm needs to be modified to produce both 1-minute and 5-minute-cadence fluxes.
2. The noisy background is smoothed using a running average – the technique that is used in the Event Detection algorithm. A running average reduces the noise but also has a delayed rise with respect to the event itself. We have found empirically that the sum of a running average and three times the square root of the running variance reacts rapidly to an event rise while suppressing noise. The choice of the time constant for this running average has to be a balance between its ability to respond to an event onset and its ability to suppress noise (false positives).
3. A normalized backward first difference of the running average is calculated. This normalization removes the dependence on the flux level at onset. This backward first difference is compared to a criterion derived from the minimum rate-of-rise that is of concern.
4. An exponential fit is performed (in fact, a linear fit to the logarithm of the integral fluxes) to the first 3 or more points after event onset.

Since the purpose of the rate-of-rise calculation is to alert SWFO to rapidly rising events, the algorithm should operate on 1-minute or faster data. At the PDR, SWFO representatives stated that a 1-minute cadence is sufficiently fast.

SWPC characterizes SPEs primarily in terms of the >10 MeV integral flux. However, the >30 MeV and >100 MeV fluxes provide a better indicator of whether the event presents a risk to electronics [O'Brien, 2009] and humans in space, respectively. Since there is currently no solar radiation storm scale (SRSS) for >30 MeV fluxes, projected fluxes based on a >30 MeV rate-of-rise cannot be compared to a set scale. Therefore, the baseline for this algorithm is to calculate the rate-of-rise for >10 and >100 MeV fluxes. In some cases, there may be a rate-of-rise reported for the >10 MeV fluxes but no >100 MeV fluxes above the galactic cosmic ray background.

3.2 Processing Outline

At each 1-minute cadence, separately for >10 MeV and >100 MeV integral fluxes:

1. Initialize or update running average and variance
2. Calculate the ratio of the current to previous minute's running average plus three-sigma
3. Compare this ratio to a fixed criterion based on the slowest rise time to which SWFO wishes to be alerted
4. If 4 points in a row are greater than the fixed criterion, calculate a 4 -point exponential fit to the integral fluxes (not the running average)
5. Using the results of this fit, predict the time it will take to reach the SRSS flux levels.

All output predictions are tagged with the time stamp of the latest integral flux value used in the predictions, minus half a minute due to the inherent lag in a 1-minute average.

3.3 Algorithm Input

The inputs to the algorithm consist of L2+ Integral Fluxes on a 1-min cadence.

3.3.1 Primary Data

The input Level 2 Integral Flux quantities for a single SGPS are defined in Table 1. The input files for both SGPSs (+X and –X) have similar contents. The Differential-to-Integral Flux L2 product is calculated for both SGPS FOVs (eastward- and westward-looking). The orientation is determined at an earlier processing stage and input as a string ('W' or 'E') that is passed through to the output file along with the satellite ID.

Table 1. Level 2 Integral Flux inputs to SEISS Solar Proton Event Rate-of-Rise algorithm. This is for each SGPS (–X and +X).

Data Type	Refresh	Number of values	Units
Satellite ID	1 min	1	String (e.g., 'G16')
Orientation of SGPS, –X or +X	1 min	1	String (e.g., 'W' or 'E')
Integral Proton Fluxes, SGPS –X or +X	1 min	2, at >10 MeV and >100 MeV	protons / (cm^2 s sr)
Time	1 min	1 (start of period)	String (ISO 8601 format, e.g. "2016-09-09T14:30:00Z")

3.3.2 Ancillary Data

No ancillary data are required by the algorithm.

3.4 Theoretical Description

3.4.1 Physics of the Problem

The greatest levels of >1 MeV proton fluxes at geosynchronous orbit are observed during solar energetic particle (SEP) events. These energetic protons (as well as electrons and heavy ions) are believed to originate in shocks and magnetic field reconnections associated with coronal mass ejections (CME) [Cane and Lario, 2006]. The measurement of integral proton fluxes at geosynchronous orbit has both operational and scientific applications. These fluxes are sufficiently energetic to present a hazard to satellites in the region, causing undesired transient responses and single-event upsets and permanent damage in solid state devices and solar arrays, and the energy thresholds can be related to levels of shielding [Baker, 1996; O'Brien, 2009]. The proton flux observations also support alerts and warnings of radiation hazards to occupants of manned spacecraft and polar-crossing aircraft [Baker, 1996].

Integral flux is an estimate of the directional flux of particles above a certain energy threshold. Integral flux is expressed in units of protons / (cm^2 s sr), a quantity also referred to as a particle flux unit (pfu). The integral flux is reported at threshold energies of 1, 5, 10, 30, 50, 60 and 100 MeV. Using the legacy Event Detection algorithm, SWPC identifies the start of a solar proton event as the first of three consecutive 5 minute averages of the >10 MeV integral flux that are greater than or equal to 10 pfu, and issues an S1 alert. Higher levels of alerts are issued when the >10 MeV integral flux exceeds 100 (S2), 1000 (S3), 10,000 (S4), and 100,000 (S5) pfu [Poppe, 2000]. An alert is also

issued when the >100 MeV integral flux exceeds 1 pfu, which is a better indicator of radiation risk to aircraft passenger and crews at high latitudes than the >10 MeV alerts. The input GOES R L1b data have a 1 minute latency requirement due to the rapidity with which an SEP event can reach its peak level after triggering the initial alert. In such rapid cases, the legacy Event Detection algorithm may be too slow to permit adequate alerts. The purpose of the Rate-of-Rise algorithm is to supplement the Event Detection algorithm in such cases.

The rising phase of a solar proton event (SPE) is approximately exponential in time. This fact has been used previously in characterizing the initial increase in solar proton fluxes [Posner, 2007]. Therefore, in this algorithm, the rates-of-rise are characterized using an exponential model.

3.4.2 Mathematical Description

Background Estimate

Solar proton events are detected as they rise out of the instrument backgrounds. Backgrounds are due to in-band galactic cosmic ray protons as well as contamination due to out-of-band or out-of-field protons. Because backgrounds vary, they are characterized by a running average and a standard deviation (more precisely, the square root of the running variance).

The running average method is similar to that used on GOES 8-15 solar proton measurements, except that here it is applied to the 1-minute integral fluxes rather than the 5-minute channel fluxes. The running average is based on n = 30 minutes of data. (The time constant n is selected to provide a balance between too many false positives and too slow of a response to SPE onsets.)

The method used is a recursive filter with time constant n = 30 minutes and a sample period (1 min) much less than the time constant [Enochson and Otnes, 1968, p. 57]. (It is analogous to the simplest kind of low-pass filter, made of a resistor (R) and a capacitor (C) in series with the time constant n = RC.) Instead of requiring that 30 minutes of data be saved, the running average is updated with every subsequent measurement:

$$\overline{J_i}(\tau) = \overline{J_i}(\tau - 1) + \frac{1}{n}\left[J_i(\tau) - \overline{J_i}(\tau - 1)\right] \tag{1}$$

where J_i is the integral flux for energy threshold i, τ is the current reporting period and τ-1 is the previous reporting period, and n is the number of samples (for 1-minute cadence, n = 30).

The standard deviation of the background must also be calculated. Since the integral fluxes are a complicated function of the original channel counts, a simple expression based on Poisson statistics is not possible. Rather, the algorithm updates the variance of the background over the same period that the running average is calculated. The running variance for the flux J_i at reporting period τ is given by [Enochson and Otnes, 1968, p. 238]

$$z_i(\tau) = \frac{1}{n} J_i^2(\tau) + \left(\frac{n-1}{n}\right) z_i(\tau - 1) \tag{2}$$

$$\overline{\sigma_i^2}(\tau) = z_i(\tau) - \overline{J_i}^2(\tau) \tag{3}$$

The standard deviation is calculated as the square root of the running variance. The running averages and variances calculated from these expressions agree well (though somewhat smoothed, which is desirable in this application) with averages and variances calculated using all points in the 30-minute period simultaneously. Both calculations require a 'seed' value for the average flux and variance, which must be determined empirically from on-orbit values.

Initializing Running Mean and Variance

The above expressions for running mean and variance require that the prior running mean, $J_i(\tau\text{-}1)$, and the prior value of z, $z_i(\tau\text{-}1)$, be initialized whenever the algorithm software is started. Fixed initial values can be defined, but since the background levels vary, this may cause a discrepancy between the given initial values and 'true' values of J_i and z_i. If the initial values are far from the 'true' values, there will be a transient that dies off over a period that depends on the initial discrepancy. However, even a short artificial transient can cause problems. Therefore, the running mean and variance are initialized using the first value read in, $J_i(0)$.

The initial value of the running mean is given by

$$\overline{J_i}(-1) = J_i(0) \tag{4}$$

and, therefore, the running mean at τ = 0 is given by

$$\overline{J_i}(0) = J_i(0) \tag{5}$$

This expression is for illustrative purposes; in the actual calculations, the more general expression given above is used with the initial value given above.

Then, the question is how to estimate the initial running variance, given the above expression and

$$z_i(\tau) = \overline{\sigma_i^2}(\tau) + \overline{J_i}^2(\tau) \tag{6}$$

Since the integral fluxes are complicated functions of the measured channel fluxes, we cannot use Poisson statistics straightforwardly to calculate an initial estimate for the variance. Rather, we determine empirically that for the GOES >10, >30, >60 and >100 MeV proton fluxes, the square root of the running variance is approximately half of the running average. It varies from ~0.4 to ~0.6, depending on the energy and the year; this proportional factor is a patchable constant η (Table 6). Therefore, the initial value of z_i is given by:

$$z_i(-1) = \left(1+\eta^2\right)J_i^2(0) = 1.25J_i^2(0) \tag{7}$$

and, therefore, the value of z_i at $\tau = 0$ is given by

$$z_i(0) = \frac{1+1.25(n-1)}{n} J_i^2(0) \tag{8}$$

Again, this expression is for illustrative purposes; in the actual calculations, the more general expression given above is used with the initial value given above.

Onset Detection Criterion

The initial guess is based on f_{run}, the running average plus the product of an empirical factor q and sigma (currently, q = 3):

$$f_{run}(\tau) = \overline{J_i}(\tau) + q\sqrt{\overline{\sigma_i^2}(\tau)} \tag{9}$$

We look for a rapid change in this quantity using a backward difference as an estimate of the first derivative [Milne, 1970, p. 49]:

$$\nabla f_{run}(\tau) = f_{run}(\tau) - f_{run}(\tau-1) \tag{10}$$

The use of this quantity both normalized and unnormalized was considered. Because of the wide dynamic range involved in SPE fluxes, it was found that a normalized criterion was simpler to implement. The normalized criterion is based on whether the normalized backwards difference is greater than some fraction ε (channel-dependent) of $f_{run}(\tau-1)$, or equivalently:

$$\frac{f_{run}(\tau)}{f_{run}(\tau-1)} > 1+\varepsilon \tag{11}$$

The criterion ε or its equivalent is derived based on an exponential decade rise in flux within a specified amount of time by equating $J(\tau) = a\exp(b\tau)$ with $f_{run}(\tau)$. Then, the following expression is straightforward to derive:

$$b = \ln\left(\frac{f_{run}(\tau)}{f_{run}(\tau-1)}\right) \tag{12}$$

A value of b = 1 min^{-1} predicts a decade flux increase in 2.3 minutes. Having estimated b from the observations, if we define the maximum time Δt_{10} it takes for the flux to rise a decade (for example, 30 minutes), then b can be used to determine whether the event is rising sufficiently quickly:

$$b \geq \frac{\ln 10}{\Delta t_{10}} \tag{13}$$

Or equivalently,

$$\frac{f_{run}(\tau)}{f_{run}(\tau-1)} \geq \exp\left(\frac{\ln 10}{\Delta t_{10}}\right) \tag{14}$$

This is the criterion for performing a fit and for reporting a first guess (see below for both of these calculations), given Δt_{10}. Setting this time requires a balance between missing some truly rapidly rising events and too many false positives. Initial testing indicates that 30 minutes is a good value, reinforced by requiring m = 4 of these in a row before a fit is performed. According to this formulation, there is no need to calculate ε itself operationally, but for Δt_{10} = 30 min, ε = 0.080 (and b = 0.077 min^{-1}, 1/b = 13 min).

Curve Fits

If the criterion derived above is satisfied for m consecutive points, then we fit an exponential to the n points of the 1-minute integral flux at t = τ–(m–1), τ–(m–2),…,τ –1, τ. (This implies that at all times we must save the m–1 previous points.) The exponential expression is given by

$$J(t-\tau) = a(\tau)\exp[b(\tau)(t-\tau)] \tag{15}$$

where the exponential time constant is 1/b. This indicates that a new fit is performed at each subsequent t while the backward difference condition holds. The fit is performed as a linear fit [Press et al., 1988, p. 524] to the natural logarithm of this expression:

$$\ln[J(t-\tau)] = \ln[a(\tau)] + b(\tau)(t-\tau) = A_0(\tau) + A_1(\tau)(t-\tau) \tag{16}$$

The fit parameters A_0 and A_1 vary with time during the rise of a single event. These results are used to predict when the event will reach the NOAA solar radiation storm scale thresholds (J_{scale}),

$$\Delta t(t-\tau, J_{scale}) = \frac{\ln J_{scale} - A_0(t-\tau)}{A_1(t-\tau)} - \Delta t_L \tag{17}$$

The constant Δt_L should be set to at least half the intersample spacing (0.5 min) in order to account for the inherent delay in calculating a 1-minute average. It can also account for the total latency of the system if this is known. If a fit results in a b (equation 13) that is greater than the value corresponding to Δt_{10} = 30 min (b = 0.077 min^{-1}, 1/b = 13 min), the resulting projected time is not reported in the output.

It may be tempting to calculate a similar projected time from the backward differences using an exponential model and to report these as initial guesses. However, based on calculations with 1-min integral flux proxy data, this would result in ~16,000 false positives per year from the >10 MeV flux (~22,000 from the >100 MeV flux). Waiting for m = 4 consecutive points satisfying the criterion is essential for reducing the number of false positives to an acceptable level.

SGPS Orientation

This is a pass-through value from the SEISS.18 Integral Flux product to the Rate-of-Rise output. The identification of the eastward (E) or westward (W) orientation of the SGPS –

X and +X units is determined at an earlier processing stage. The event detection is performed separately on the data from each SGPS unit. In the unlikely event that a yaw flip takes place during the rise of a SEP event, the flags will indicate that the assessment of the event is mixed between the two directions. (The event detection algorithm does not 'switch' between the two units in real time.) If so, the assessment should be redone off-line for archival purposes.

3.4.3 Algorithm Output

The outputs of the Rate-of-Rise algorithm are summarized in Table 2. An output is provided only if the algorithm detects a sufficiently rapid rise. These results are reported in an ASCII format for immediate use by the forecast office (Figure 3 and Figure 4). There is a separate ASCII file for each energy (10 or 100 MeV). When one of these files is opened, the 'log_file_open' flag is set to 1. If this flag is set, the algorithm starts counting if a fit does not take place at a given 1-minute interval. Once this count reaches 1440, the log file is closed and the flag is reset to 0.

Table 2. Level 2 Outputs of SEISS Solar Proton Event Rate-of-Rise Algorithm. This is for each SGPS (–X and +X).

Data Type	Refresh	Number of values	Units
Satellite ID and Orientation of SGPS, –X or +X	1 min	1	String (e.g., 'G16 Sensor Orientation: W')
Time-tag of latest integral flux used in prediction	1 min	1	String (ISO 8601 format, e.g. "2016-09-09T14:30:00Z")
Predicted time for $J_{>10MeV}$ to reach 10^1 pfu (S1)	1 min	1	minutes
Predicted time for $J_{>10MeV}$ to reach 10^2 pfu (S2)	1 min	1	minutes
Predicted time for $J_{>10MeV}$ to reach 10^3 pfu (S3)	1 min	1	minutes
Predicted time for $J_{>10MeV}$ to reach 10^4 pfu (S4)	1 min	1	minutes
Predicted time for $J_{>10MeV}$ to reach 10^5 pfu (S5)	1 min	1	minutes
Predicted time for $J_{>100MeV}$ to reach 10^0 pfu	1 min	1	minutes
Predicted time for $J_{>100MeV}$ to reach 10^1 pfu	1 min	1	minutes
Predicted time for $J_{>100MeV}$ to reach 10^2 pfu	1 min	1	minutes

Data Type	**Refresh**	**Number of values**	**Units**
Predicted time for $J_{>100MeV}$ to reach 10^3 pfu	1 min	1	minutes

```
G08 Sensor Orientation: W
UT                  dt(J>10=1e1) dt(J>10=1e2) dt(J>10=1e3) dt(J>10=1e4) dt(J>10=1e5)
2000-07-14T10:45Z     1.9 min     16.7 min     31.4 min     46.2 min     61.0 min
2000-07-14T10:46Z     0.8 min     15.2 min     29.7 min     44.2 min     58.7 min
2000-07-14T10:47Z    -----         6.3 min     13.8 min     21.4 min     28.9 min
2000-07-14T10:48Z    -----        15.3 min     32.3 min     49.3 min     66.3 min
2000-07-14T10:49Z    -----        10.4 min     23.6 min     36.8 min     50.0 min
2000-07-14T10:50Z    -----         8.7 min     21.4 min     34.2 min     46.9 min
2000-07-14T10:51Z    -----         3.7 min     11.2 min     18.6 min     26.1 min
2000-07-14T10:52Z    -----         4.2 min     13.9 min     23.6 min     33.4 min
2000-07-14T10:53Z    -----         6.3 min     21.2 min     36.1 min     50.9 min
2000-07-14T10:54Z    -----         5.7 min     21.5 min     37.4 min     53.3 min
2000-07-14T10:55Z    -----         5.8 min     24.2 min     42.5 min     60.9 min
2000-07-14T10:56Z    -----         3.4 min     18.1 min     32.7 min     47.3 min
2000-07-14T10:57Z    -----         5.4 min     29.3 min     53.2 min     77.0 min
2000-07-14T10:58Z    -----         4.6 min     28.5 min     52.5 min     76.4 min
2000-07-14T10:59Z    -----         4.7 min     33.6 min     62.6 min     91.5 min
2000-07-14T11:00Z    -----         2.5 min     25.8 min     49.1 min     72.4 min
2000-07-14T11:01Z    -----         1.2 min     22.5 min     43.8 min     65.2 min
2000-07-14T11:02Z    -----        -----        -----        -----        -----
```

Figure 3. Example of a proxy output file for the onset of the Bastille Day 2000 event at >10 MeV.

```
G08 Sensor Orientation: W
UT                  dt(J100=1e0) dt(J100=1e1) dt(J100=1e2) dt(J100=1e3)
2000-07-14T10:39Z    -----         4.7 min      9.7 min     14.7 min     -----
2000-07-14T10:40Z    -----         5.6 min     12.0 min     18.5 min     -----
2000-07-14T10:41Z    -----         8.7 min     19.2 min     29.7 min     -----
2000-07-14T10:42Z    -----         4.3 min     11.2 min     18.0 min     -----
2000-07-14T10:43Z    -----         4.3 min     12.5 min     20.7 min     -----
2000-07-14T10:44Z    -----         2.7 min     10.0 min     17.3 min     -----
2000-07-14T10:45Z    -----         2.3 min     10.4 min     18.6 min     -----
2000-07-14T10:46Z    -----         1.5 min     10.2 min     18.8 min     -----
2000-07-14T10:47Z    -----         0.4 min      9.1 min     17.8 min     -----
2000-07-14T10:48Z    -----        -----         7.6 min     15.8 min     -----
2000-07-14T10:49Z    -----        -----         7.9 min     17.4 min     -----
2000-07-14T10:50Z    -----        -----         8.6 min     19.7 min     -----
2000-07-14T10:51Z    -----        -----         7.4 min     18.2 min     -----
2000-07-14T10:52Z    -----        -----         6.8 min     18.3 min     -----
2000-07-14T10:53Z    -----        -----         7.3 min     20.6 min     -----
2000-07-14T10:54Z    -----        -----         7.1 min     21.8 min     -----
2000-07-14T10:55Z    -----        -----         6.7 min     22.4 min     -----
2000-07-14T10:56Z    -----        -----         6.7 min     24.2 min     -----
2000-07-14T10:57Z    -----        -----         8.3 min     31.3 min     -----
2000-07-14T10:58Z    -----        -----         9.7 min     38.5 min     -----
2000-07-14T10:59Z    -----        -----         8.4 min     36.4 min     -----
2000-07-14T11:00Z    -----        -----         7.1 min     34.5 min     -----
2000-07-14T11:01Z    -----        -----        -----        -----        -----
2000-07-14T11:02Z    -----        -----        -----        -----        -----
2000-07-14T11:03Z    -----        -----        -----        -----        -----
```

Figure 4. Example of a proxy output file for the onset of the Bastille Day 2000 event at >100 MeV.

4.0 TEST DATA SETS AND OUTPUTS

4.1 Simulated/Proxy Input Data Sets

Integral fluxes are not produced at 1-minute cadence by the current (GOES-13-15) or the previous (GOES 8-12) processing system. Therefore, proxy 1-minute integral fluxes are produced by removing the background from the 1-minute channels fluxes using a running average, performing the Zwickl [1989] contamination correction on 1-minute channel fluxes, and calculating integral flux using the GOES-R L2+ algorithm.

The algorithm for removing the background is new and therefore is described here. It was developed in order to avoid the jumps that occur every ten days in the current background correction. It is based on the calculation of a 4-hr running average and standard deviation of the channel fluxes. Qualitatively, the goal is to use this running average as the background unless an SPE is underway, in which case the background is frozen to the value prior to the SPE onset. An SPE onset is defined as an increase in the time-derivative of the flux (approximated by a backward difference) above an empirical threshold that is channel-dependent (Table 3).

Table 3. Parameters Used in Removal of Backgrounds from 1-min Channel Fluxes

Channel	P2	P3	P4	P5	P6	P7
Backward Difference Threshold (cm^{-2} s^{-1} sr^{-1} MeV^{-1})	0.0008	0.0008	0.0001	0.00005	0.00001	0.000005
Recapture Fraction	0.005	0.005	0.01	0.01	0.01	0.01

Every minute, the running quantities are updated and a backward difference is calculated from the current and previous 1-min flux averages. If this backward difference is less than some threshold, the background is updated with the new running average, as is a quantity called the ‘base’, which is 1/5 the running standard deviation. (This is similar to a static quantity used by the Zwickl [1989] model.) If the backward difference is greater than this threshold, the background level is frozen at the prior level until the difference between the running average and the frozen background level, normalized to the background, is less than some specified ‘recapture’ fraction (Table 3). (Note that no background is removed from the P1 fluxes since there are almost always trapped radiation belt protons in this energy range.)

One potential drawback of this method is that it may remove weak, slowly-rising SPEs as well as Forbush decreases in the background levels. However, the purpose of the background-corrected fluxes is to identify large SPEs; users desiring to study weak SPEs or Forbush decreases should refer to the uncorrected fluxes.

The sources of the proxy data are summarized in Table 4.

Table 4. Sources of Rate-of-Rise 1-minute Proxy Data

Start Date	Stop Date	Satellite
1995.01.01	2003.06.30	GOES-8
2003.07.01	2006.06.30	GOES-12 (P1-P5) + GOES-11 (P6-P7)
2006.07.01	2010.12.31	GOES-11

The reason for combining GOES-12 and GOES-11 data between July 2003 and June 2006 is as follows. During this period, GOES-11 was spinning in storage mode yet its 5-minute solar proton observations were used by the Forecast Center because channels P6 and P7 from GOES-12 had failed. At first we tried to use the 1-min fluxes from GOES-11 during this period as proxy data, but we found a surprisingly large number of spikes in the data. On further examination, we found that these 'spikes' were in fact oscillations in the observed fluxes at 1-minute resolution (Figure 5). These oscillations are much reduced in the 5-minute GOES-11 data. They are due to the satellite spin in the presence of flux anisotropies such as those reported by Rodriguez et al. [2010] and generally lie between the westward- (GOES-12) and eastward- (GOES-10) observed fluxes since the eastward geomagnetic cutoffs are among the highest and the westward cutoffs are among the lowest for observations at GOES [Kress et al., 2013]. These oscillations make the spinning GOES-11 data unsuitable for proxy data for this algorithm.

In order to synthesize proxy data for this period, which includes the canonical 20 January 2005 event, we supplement the P1-P5 channels from GOES-12 with P6 and P7 from GOES-11. These two highest energy channels are relatively immune to the spinning motion of GOES-11 because their energies lie above most geomagnetic cutoffs and because these two channels are strongly bi-directional in their responses. The >10 and >100 MeV fluxes calculated from these proxy data for the 20 January 2005 event are shown in Figure 6. Those calculated from the background- and contamination-corrected fluxes agree well with the 5-minute GOES-11 integral fluxes calculated by SWPC.

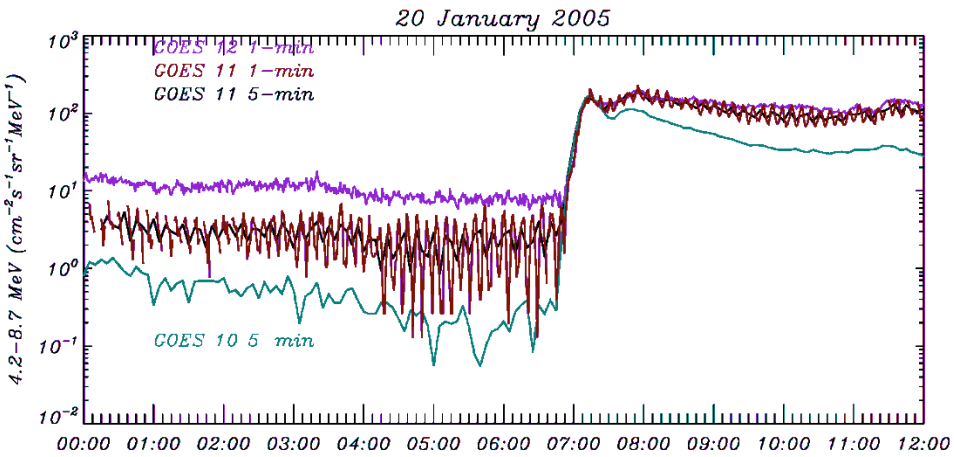

Figure 5. Comparison of eastward-observed (GOES-10) and westward-observed (GOES-12) fluxes with those observed from a spinning satellite (GOES-11). Observations are from the P2 (4.2-8.7 MeV) GOES channel. The oscillations in the GOES-11 fluxes are signatures of the flux anisotropies that result in the large differences between the GOES-10 and GOES-12 fluxes.

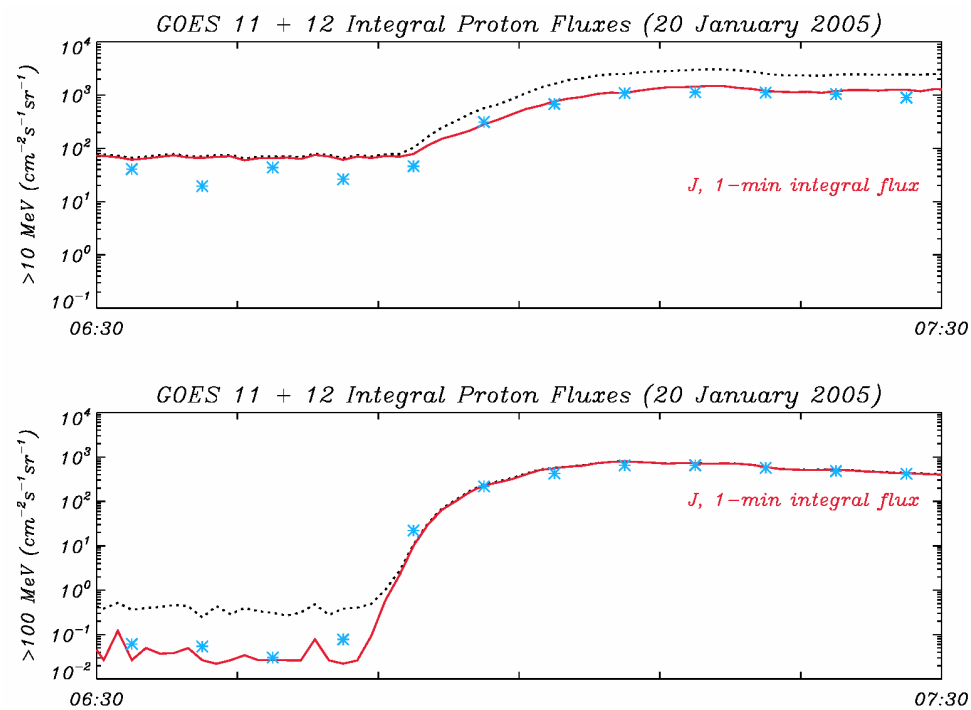

Figure 6. Integral fluxes during the rise of the 20 January 2005 event. The red traces are the proxy data calculated from the 1-min GOES-12 and GOES-11 data after removal of backgrounds and contamination. The black dotted traces indicate the results without removal of the backgrounds and contamination. The blue stars are the 5-min GOES-11 integral fluxes. The lower 5-min GOES-11 >10 MeV fluxes prior to event onset are due to the anisotropy averaging shown in Figure 5.

4.2 Test Results Using Proxy Input Data

The rate-of-rise algorithm has been run on proxy data covering January 1, 1995 through December 31, 2010, including Solar Cycle 23. There are a few data gaps (in particular during the first half of 2003) but no SPEs are missing. The criterion used was a projected exponential rise of a decade in 30 minutes or less. (If this criterion is reduced, then fewer events will be identified.) There were 33 rapidly-rising events detected in this manner; 15 were detected in both energy ranges, 13 at >10 MeV only and 5 at >100 MeV only. These events are listed in Table 5, identified by their onset dates and times (onset being the first time at which there had been four consecutive points above the criterion). They include the Bastille Day 2000 event and the Halloween 2003 events.Events with breaks less than an hour are counted as single event.

Table 5. Rapidly-rising events during Solar Cycle 23 and their onset times (UT) at each energy.

Event Date	>10 MeV	>100 MeV	Event Date	>10 MeV	>100 MeV
1997.11.06	12:58	12:39	2002.02.20	07:03	---
1998.05.02	14:03	14:02	2002.04.21	---	01:48
1998.05.06	08:29	08:26	2002.08.08	---	13:59
1998.09.25	00:25	---	2002.08.24	01:34	01:30
1998.09.30	---	14:28	2003.10.26	18:19	18:08
1998.11.14	08:11	---	2003.10.28	12:27	11:39
2000.06.10	17:51	---	2003.10.29	---	21:15
2000.07.14	10:45	10:39	2003.11.02	---	17:42
2000.11.08	23:39	23:52	2004.11.07	18:59	---
2001.04.03	00:44	---	2004.11.10	05:30	---
2001.04.15	14:05	14:03	2004.11.10	16:35	---
2001.04.28	04:59	---	2005.01.17	14:20	---
2001.08.16	01:37	00:45	2005.01.20	06:56	06:53
2001.09.15	14:32	---	2005.05.15	01:46	---
2001.11.04	16:57	16:49	2006.12.13	03:18	02:54
2001.12.26	06:00	05:53	2006.12.14	23:18	22:48
2001.12.29	08:18	---			

Selected events are plotted in Figure 7 through Figure 11. Figure 7 shows the results for the 20 January 2005 event. Both the >10 MeV and >100 MeV fluxes rise sufficiently rapidly to meet the criterion, as in the Bastille Day 200 event (Figure 9) and the 13 Dec 2006 event (Figure 11). The 02 November 2003 event (last in the Halloween 2003 series) only satisfies the criterion in the >100 MeV flux (Figure 10). In contrast to these famous event, Figure 8 is an example of a weak event that reached only the S1 level on the Solar Radiation Storm Scale. It satisfies the rapid-rise criterion for a few points in the >10 MeV flux, but the first exponential curve fit has a time constant that is too long, due to the first point in the fit being greater than the subsequent points. Such cases can be handled by rejecting any curve fits whose time constants are greater than the equivalent to the backwards-difference criterion (in this case, 13 minutes).

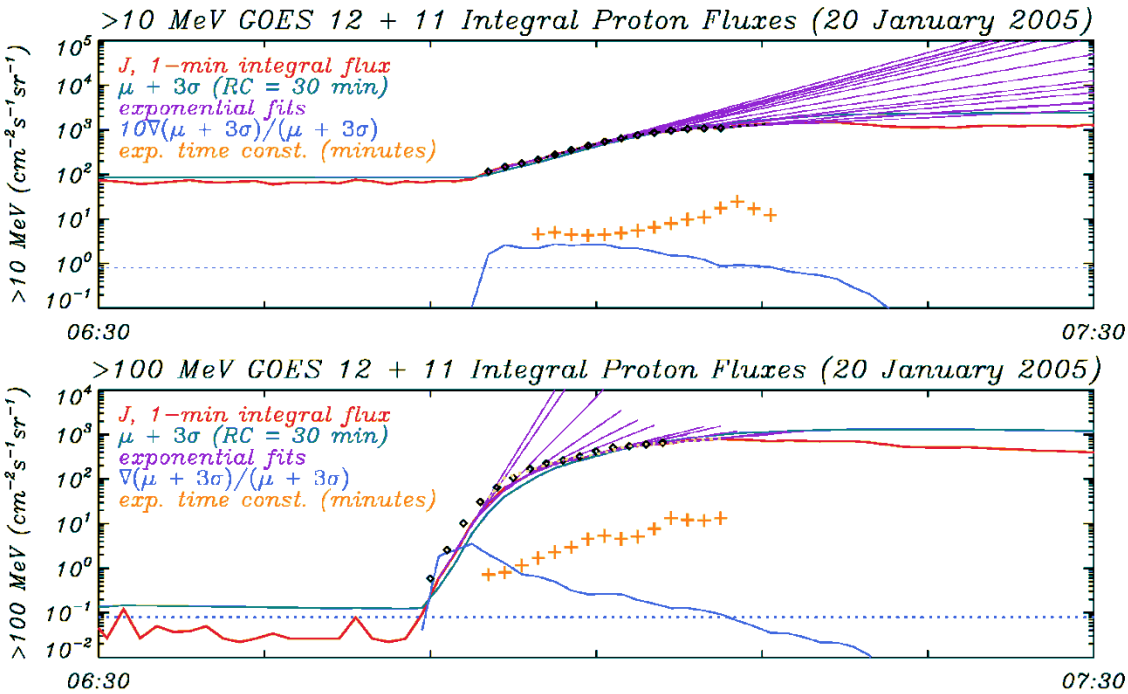

Figure 7. Rate-of-rise calculations for the 20 January 2005 event. The red trace is the 1-minute integral flux calculated by the L2 Integral Flux algorithm. The green trace is the running mean plus 3 sigma, which is used to detect a rapid rise in the presence of noise. The blue trace is the normalized backwards difference calculated from the running mean plus 3 sigma (the dashed blue trace is the criterion). The purple lines are the exponential fits to 4 consecutive points that meet or exceed the criterion, and the orange crosses are the corresponding time constants in minutes.

During this 16-year period, there were 10 false positives, or 1.25 false positives every two years. The false positives are caused when there are 4 or more samples in a row that exceed the backward-difference criterion but are not at the onset of (or during) a SPE. One false positive in this set was caused by an artifact of the background removal algorithm (due to a large stray spike). The number of false positives could be reduced by increasing the minimum number of points to 5, at a cost of 1 minute of advance warning.

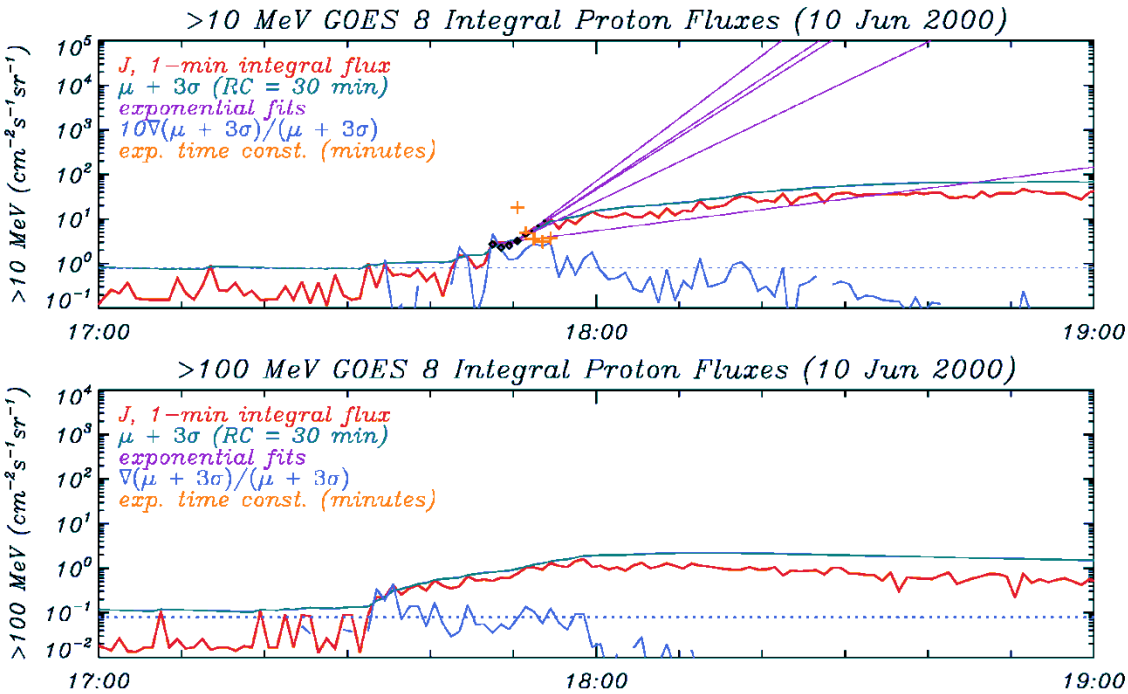

Figure 8. Rate-of-rise calculation for the 10 June 2000 event. See Figure 7 caption for explanation.

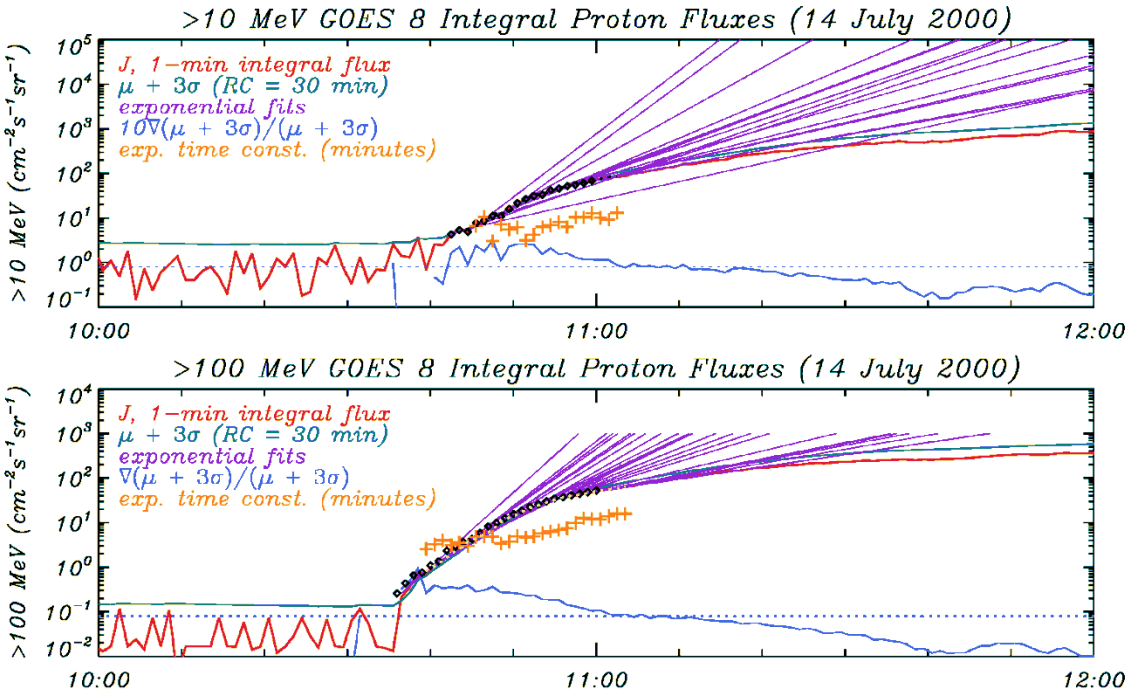

Figure 9. Rate-of-rise calculation for the 14 July 2000 event. See Figure 7 caption for explanation.

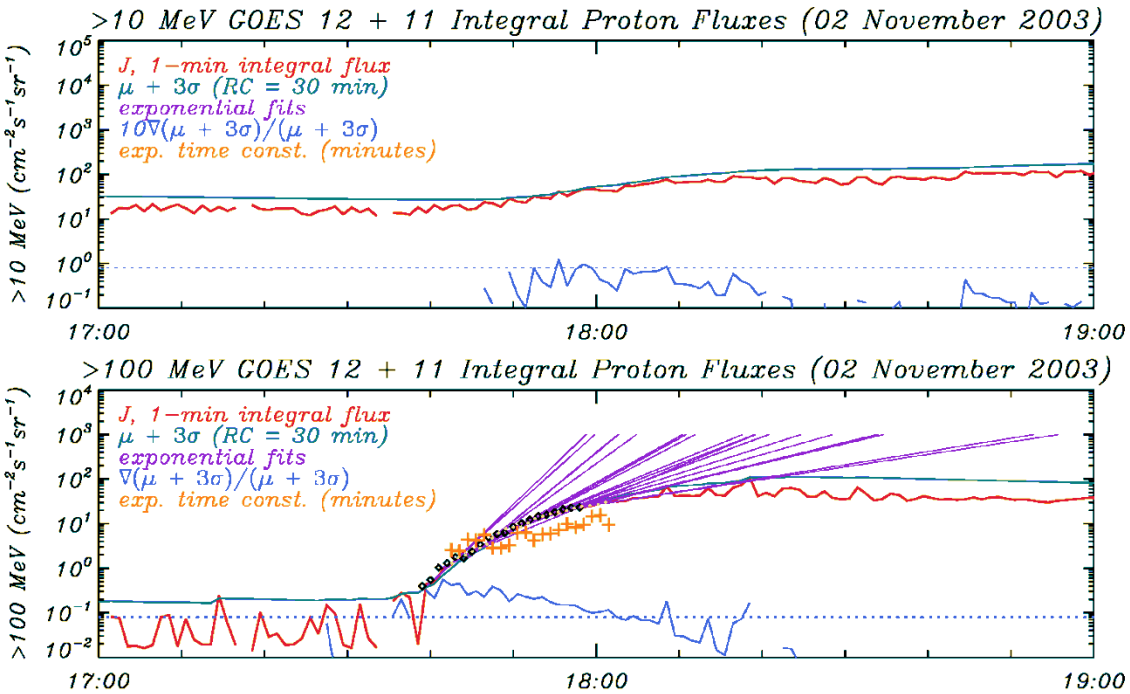

Figure 10. Rate-of-rise calculation for the 2 Nov 2003 event. See Figure 7 caption for explanation.

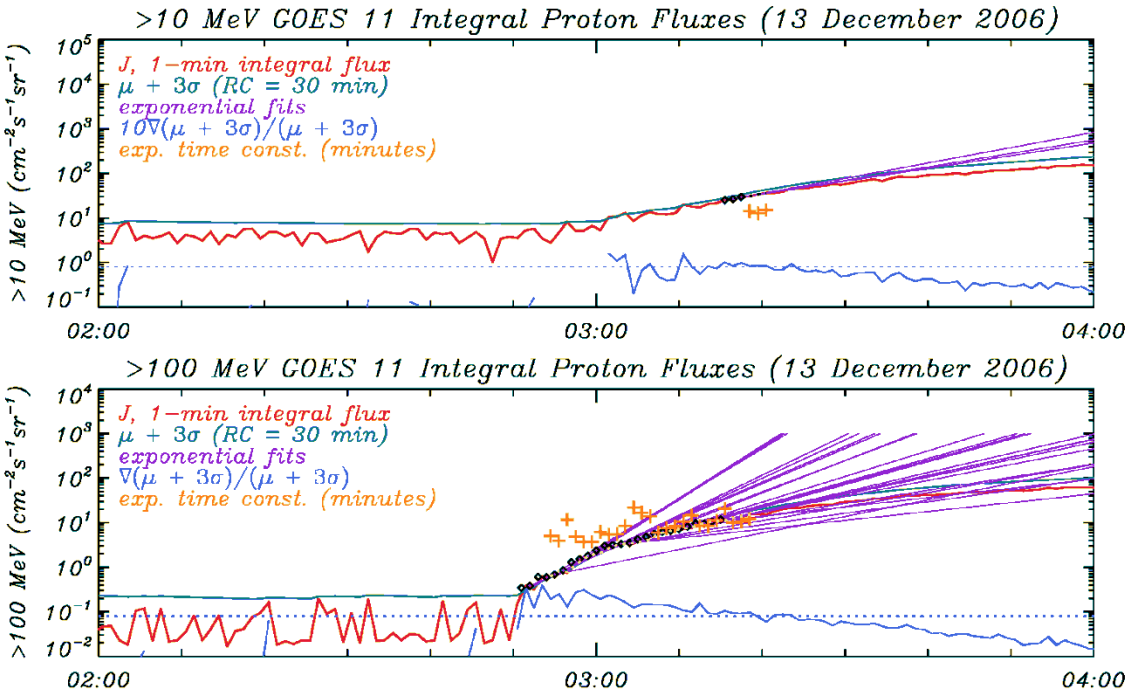

Figure 11. Rate-of-rise calculation for the 13 Dec 2006 event. See Figure 7 caption for explanation.

Similar plots are shown in Figure 12 and Figure 13 for the October 1989 SPE. This event is well-known as the largest SPE observed (in terms of >10 MeV event fluence) at least since the August 1972 event, possibly during the space age [Tylka et al., 1997] and is used to define an extreme SPE for satellite designers. However, it was characterized as well by rapid rates-of-rise in the >10 MeV and >100 MeV fluxes, both at the event onset (19 October, Figure 12) and at the onset of a superposed event on 22 October (>100 MeV fluxes only, Figure 13). In order to calculate these 1-minute integral fluxes, GOES-7 full-resolution count rates (3-sec accumulation period, 50%, 25% or 12.5% duty-cycles depending on channel energy) were averaged and converted to fluxes using the geometrical factors used currently by SWPC in real-time processing, then corrected for contamination using the Zwickl [1989] algorithm. Integral fluxes were calculated from these corrected and averaged channel fluxes using the GOES-R Integral Flux algorithm.

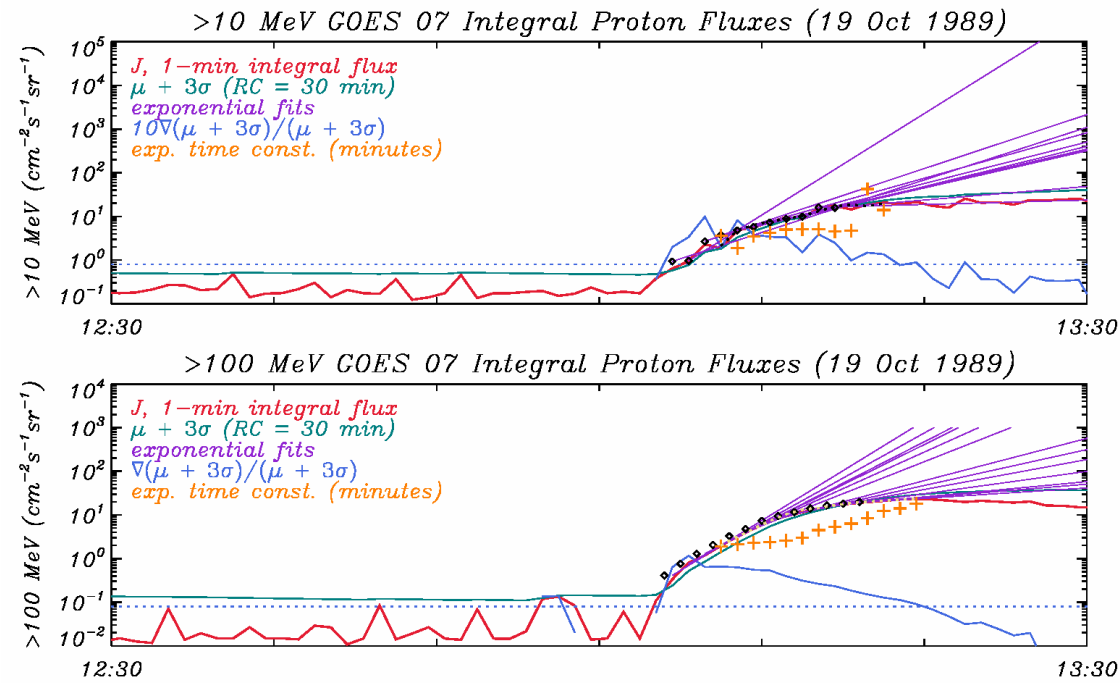

Figure 12. Rate-of-rise calculation for the 19 Oct 1989 event. See Figure 7 caption for explanation.

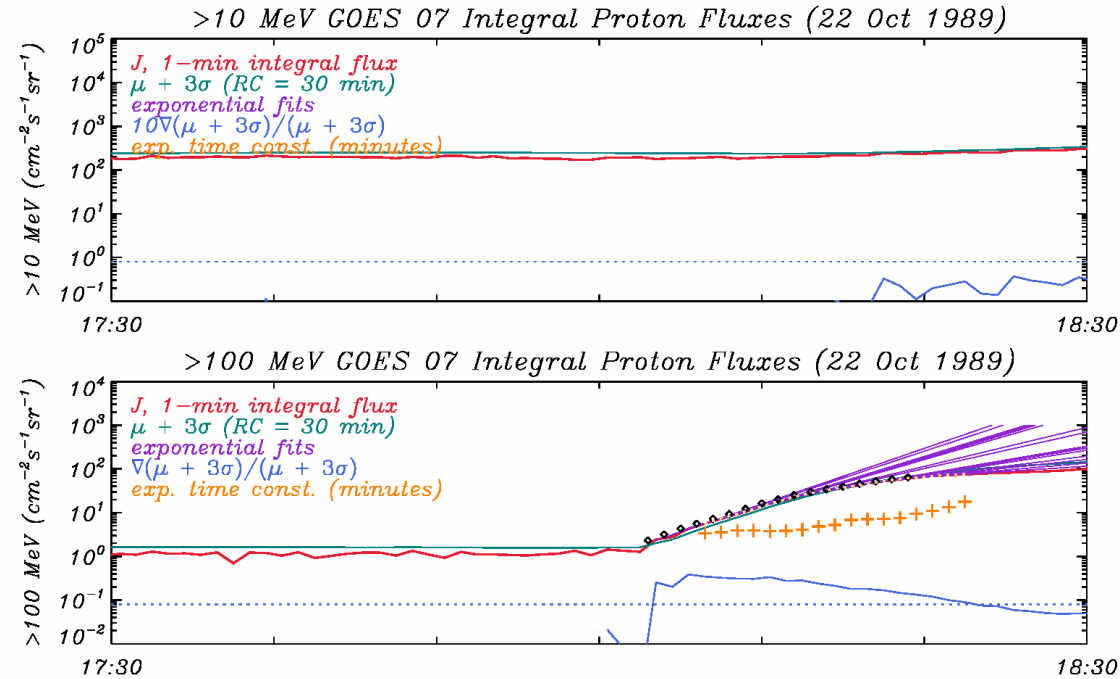

Figure 13. Rate-of-rise calculation for the 22 Oct 1989 event. See Figure 7 caption for explanation.

5.0 PRACTICAL CONSIDERATIONS

5.1 Numerical Computation Considerations

The linear fit can be implemented without using special libraries. As with any fit, double precision is advisable.

5.2 Programming and Procedural Considerations

The real-time code has been developed in Python, consisting in two files, one containing the main program and one containing a custom library of functions for Rate-of-Rise. The algorithm relies on the history of the environmental observables. As currently implemented, the code keeps track of this history in memory.

5.3 Quality Assessment and Diagnostics

As shown in Figure 8 (10 June 2000 case), a curve fit may result in a time constant that is larger than the maximum time constant (13 minutes for the criterion $\varepsilon = 0.08$). Any estimates from such an excessive time constant are omitted from the report.

5.4 Exception Handling

No rate of rise is calculated if there is a data gap. A data gap will cause the determination of the number of consecutive points (m) that exceed the rate-of-rise criterion to be restarted, and therefore delay or prevent the determination of the predicted times to the SRSS levels. Attempting to address this by interpolating across gaps could result in an increased number of false positives.

5.5 Algorithm Validation

Following GOES-R launch, the event detection algorithm cannot be validated until the SGPS L1b fluxes have been validated against the EPEAD channel fluxes and the SGPS L2 integral fluxes have been validated against the EPEAD-derived integral fluxes. Validation requires solar proton events. If GOES-R launches other than at the peak of a solar cycle like Solar Cycle 23, it may not be possible to validate the Solar Proton Event Rate-of-Rise algorithm during post-launch test (PLT) except as to its false positive rate. See Table 6 for the constants that need to be validated post-launch.

6.0 ASSUMPTIONS AND LIMITATIONS

6.1 Constants to be Re-evaluated During Cal/Val

The configurable constants in Table 6 will have to be validated during PLT. Please refer to the section on “Mathematical Description” for how these constants are used.

Table 6. Pre-Launch Values of the Configurable Constants in Solar Proton Rate-of-Rise Algorithm

Constant	Description	>10 MeV	>100 MeV
n	Number of 1-min points in running mean	30	30
q	Multiplier of running standard deviation	3	3
η	Proportion of running standard deviation to running mean, seed value	0.5	0.5
m	Number of points in fit	4	4
ε	Criterion for backwards difference	0.08	0.08
Δt_{10}	Maximum time (minutes) for flux to rise a decade	30	30
Δt_L	Correction time (minutes) for delays in the system, including half the intersample spacing	0.5	0.5
J_{scale}	Levels to which integral flux is projected 1/(cm^2 sr s)	10, 100, 1000, 10000, 100000	1, 10, 100, 1000
Open file time limit	Maximum minutes a log file may be open	1440	1440

6.2 Input and Output File Contents and Formats

See Table 1 and Table 2 for assumed contents of the input and output files. The input L2 files are in netCDF4 format and the output files are in ASCII format, shown in Figure 3 and Figure 4.

6.3 Performance

Algorithm development by the Space Weather Algorithm Team assumes that the instrument meets the performance requirements outlined in the GOES-R MRD and SEISS PORD. In particular, it assumes that the response to out-of-band particles (including direction, energy range, and species) in any channel is no greater than 10% of the response to in-band particles, as specified by the PORD (3.2.1.5), after Level 1b processing. The out-of-band particles are primarily protons.

It is assumed that the background levels are comparable to or lower than those in the corrected GOES-8-15 fluxes, due to improved out-of-band rejection in the SGPS or to a background removal performed by the L2+ SEISS.18 Integral Flux algorithm.

6.4 Pre-Planned Product Improvements

The algorithm may be extended straightforwardly to other integral flux energies such as 30 MeV or 500 MeV, if an appropriate scale is defined.

When implemented in the operational framework, the algorithm can correct the projected times using a true latency calculated by calculating the difference between the current system time and the time stamp of the 1-minute average.

For human safety purposes, a rate-of-rise product based on 1-second-cadence L1b fluxes at ~100 MeV and higher could be investigated after GOES-R launches and the SGPS 1-second fluxes have been validated.

7.0 REFERENCES

Baker, D. N. (1996), Solar wind-magnetosphere drivers of space weather, *J. Atmos. Terr. Phys., 58*, 1509-1526.

Bevington, P. R., and D. K. Robinson (1992), *Data Reduction and Error Analysis for the Physical Sciences*, Second Edition, 328 pp, McGraw-Hill.

Cane, H. V., and D. Lario (2006), An introduction to CMEs and energetic particles, *Space Sci. Rev., 123*, 45-56.

Enochson, L. D., and R. K. Otnes (1968), *Programming and Analysis for Digital Time Series Data*, SVM-3, Shock and Vibration Information Center, US Department of Defense, 277 pp.

Kim, M-H. Y., X. Hu, and F. A. Cucinotta (2005), Effect of shielding materials from SPEs on the lunar and Mars surface, *Space 2005*, AIAA 2005-6653.

Kress, B. T., J. V. Rodriguez, J. E. Mazur, and M. Engel (2013), Modeling solar proton access to geostationary spacecraft with geomagnetic cutoffs, *Advances in Space Research, 52,* 1939–1948.

Milne, W. E. (1970), *Numerical Solution of Differential Equations*, Second Edition, New York: Dover Publications.

O'Brien, T. P. (2009), SEAES-GEO: A spacecraft environmental anomalies expert system for geosynchronous orbit, *Space Weather, 7*, 10.1029/2009SW000473.

O'Neill, P. M., Badhwar-O'Neill 2010 galactic cosmic ray flux model – revised, *IEEE Trans. Nuclear Sci., 57*, 3148-3153, 2010.

Poppe, B. B., New scales help public, technicians understand space weather, *Eos Trans. AGU, 81(29)*, pp. 322, 328, July 18, 2000.

Posner, A. (2007), Up to 1-hour forecasting of radiation hazards from solar energetic ion events with relativistic electrons, *Space Weather, 5*, S05001, doi:10.1029/2006SW000268.

Press, W. H., B. P. Flannery, S. A. Teukolsky, and W. T. Vetterling, *Numerical Recipes in C: The Art of Scientific Computing*, Cambridge University Press, 1988.

Rodriguez, J. V., T. G. Onsager, and J. E. Mazur (2010), The east-west effect in solar proton flux measurements in geostationary orbit: A new GOES capability, *Geophys. Res. Lett., 37*, L07109, doi:10.1029/2010GL042531.

Sauer, H. H., and D. C. Wilkinson (2008), Global mapping of ionospheric HF/VHF radio wave absorption due to solar energetic protons, *Space Weather, 6*, 10.1029/2008SW000399.

Tylka, Allan J., James H. Adams Jr, Paul R. Boberg, Buddy Brownstein, William F. Dietrich, Erwin O. Flueckiger, Edward L. Petersen, Margaret A. Shea, Don F. Smart, and Edward C. Smith (1997), CREME96: A revision of the cosmic ray effects on micro-electronics code, *IEEE Trans. Nuclear Science, 44,* 2150-2160.

Zwickl, R. (1989), GOES-7 Energetic Particle Algorithm, NOAA Space Environment Center, unpublished technical note.

APPENDIX A. REQUIREMENTS.

The rate-of-rise algorithm has the following requirements:

General

20.01.02 The algorithm shall operate at a cadence of 5 minutes for Event Detection and Linear Energy Transfer and 1 minute for Rate-of-Rise.

20.01.03 The algorithm shall perform all operations in less than 30 seconds.

Algorithm Inputs

20.02.01 The Event Detection and Rate-of-Rise algorithms shall ingest the integral flux outputs of the SEISS.18 Integral Flux Algorithm.

Processing

20.03.11 The algorithm shall determine the initial rate-of-rise of proton events whose integral flux is projected to increase by a factor of ten in thirty minutes or less.

20.03.12 The algorithm shall determine the initial rate-of-rise of >10 MeV and >100 MeV proton integral fluxes at a 1-minute cadence.

Algorithm Outputs

20.04.01 The Event Detection and Rate-of-Rise algorithms shall report all quantities for both the eastward- and westward-looking Solar and Galactic Proton Sensors (SGPS). *(Note: since either SGPS may look westward, depending on the yaw-flip situation, the event detection parameters need to be calculated for both directions.)*

Ancillary Data

20.06.01 The algorithm shall not ingest any ancillary data.